

On the energy dependence of the muon transfer rate from hydrogen to oxygen

S. V. Romanov^{1,*}

¹*National Research Centre "Kurchatov Institute", Moscow, 123182, Russia.*

The results of calculations of the muon transfer rate from the $1s$ state of muonic hydrogen to the nucleus of a free oxygen atom are presented in the interval of collision energies from 10^{-4} to 10 eV. The calculations were performed within a version of the perturbed stationary states method proposed earlier. The electron screening in the entrance channel of the transfer reaction was taken into account. A p -wave resonance in the transfer rate is predicted at collision energies of about 0.1 eV. This result is of interest in the context of the planned laser experiment on precise measurements of the hyperfine splitting energy of the $1s$ state of muonic hydrogen.

PACS numbers: 34.70.+e, 36.10.Ee

*This is a preprint of the Work accepted for publication in Physics of Atomic Nuclei,
© Pleiades Publishing, Ltd., 2022. <http://pleiades.online/>*

1. INTRODUCTION

The subject of the present study is the direct transfer of a negative muon μ from the $1s$ state of a muonic hydrogen atom to a nucleus of oxygen:



Here p is a proton, μO^* is a muonic oxygen atom in an excited state. Let $q(E)$ be the muon transfer rate reduced by tradition to the atomic liquid-hydrogen density of $N_{\text{H}} = 4.25 \times 10^{22} \text{ cm}^{-3}$:

$$q(E) = N_{\text{H}} v \sigma(E), \quad (2)$$

E is the collision energy, $v = \sqrt{2E/M}$ is the relative velocity of the colliding particles, M is their reduced mass, $\sigma(E)$ is the total reaction cross section summed over all final states of muonic oxygen. In an experimental study of reactions of the type of (1) in dense gaseous mixtures, the rate $\lambda(T)$ of the muon transfer from thermalized muonic hydrogen atoms is measured. It depends on the mixture temperature T and, being reduced to the density N_{H} , it is obtained by averaging the rate $q(E)$ over the Maxwellian distribution of relative velocities of the colliding particles.

The muonic hydrogen atom is an electrically neutral object whose size is two orders of magnitude less than dimensions of ordinary atoms. In this respect, it is similar to the neutron. The reaction (1) is exothermic with the excess kinetic energy of a few keV. It is well known that at low

*Romanov'SVi@nrcki.ru; Serguei.V.Romanov@gmail.com

collision energies, when the s -wave contribution predominates, the cross section of such a reaction is inversely proportional to the relative velocity: $\sigma(E) \propto 1/v$ [1]. In this case, the reaction rate $q(E)$ is independent of the collision energy, and the rate $\lambda(T)$ is independent of the temperature. The reaction (1) was experimentally studied in gaseous hydrogen–oxygen mixtures in Ref. [2]. The mixtures were kept at room temperature and under pressure from 3 to 15 bar; the oxygen concentration was a few parts per thousand. Delayed X-ray quanta emitted by muonic atoms of oxygen were observed. The time dependence of the counting rate of these quanta was found to be not purely exponential. This fact was interpreted as a manifestation of the energy dependence of the muon transfer rate at epithermal energies of $E = 0.1 - 0.2$ eV. In order to describe observed results quantitatively, the authors of Ref. [2] performed a simulation of the slowing down of muonic hydrogen atoms in gaseous mixtures with allowance for the muon transfer to oxygen. The energy dependence of the muon transfer rate $q(E)$ was assumed to be a step function. The best fit to experimental data was obtained with the following function:

$$q(E) = \begin{cases} 8.5(2) \times 10^{10} \text{ s}^{-1}, & E < 0.12 \text{ eV}; \\ 3.9 \left(\begin{smallmatrix} +0.5 \\ -1.3 \end{smallmatrix} \right) \times 10^{11} \text{ s}^{-1}, & 0.12 < E < 0.22 \text{ eV}. \end{cases} \quad (3)$$

The upper value is the rate of the muon transfer from muonic hydrogen atoms thermalized at room temperature, the lower value corresponds to epithermal energies. The epithermal transfer rate is seen to be almost five times larger. In connection with this result, the authors of Ref. [3] proposed to use the muon transfer to oxygen in a laser experiment on precise measurements of the hyperfine splitting energy of the $1s$ state of muonic hydrogen. Let us consider the idea of this experiment.

Similarly to the ordinary hydrogen atom, the energy level of the $1s$ state of muonic hydrogen is split into two components specified by values of the quantum number F of the total angular momentum. Actually, F is equal to 0 and 1, and the state with $F = 0$ has the lowest energy. The splitting energy ΔE_{1s} is mainly determined by the first-order correction of the perturbation theory in the interaction of the particle magnetic moments. In the case of the ordinary hydrogen atom, the respective result is well known [1]. The replacement of the magnetic moment of the electron by the one of the muon and taking into account the reduced mass of muonic hydrogen yield $\Delta E_{1s} \approx 0.18$ eV. The wavelength of the transition between the hyperfine components is equal to $6.8 \mu\text{m}$. Concerning the lifetime of the $1s$ state, in hydrogen with a small admixture of oxygen it is mainly determined by both the muon decay and the muon transfer to oxygen. The muon decay rate is equal to $4.5 \times 10^5 \text{ s}^{-1}$. Let us estimate the muon transfer rate. In accordance with the result (3), it is reasonable to set it equal to 10^{11} s^{-1} at the atomic liquid–hydrogen density. Then, for example, at the pressure of 40 bar and the relative oxygen concentration of 10^{-4} , the muon transfer rate becomes comparable to the muon decay rate, and the lifetime of the $1s$ state is about $1 \mu\text{s}$.

A muonic hydrogen atom in the $1s$ state is formed as a result of the cascade capture of a muon. Both the components of the hyperfine structure are populated in this process, and the kinetic energy of the muonic atom can vary within wide limits. When migrating through hydrogen gas,

the muonic atom is slowed down by losing its kinetic energy in collisions with hydrogen molecules. Moreover, the interaction of the magnetic moments of the muon and protons of molecules leads to the muon spin flip. As a result, the muonic hydrogen atom proves to be in the lower hyperfine-structure state with $F = 0$. According to results of simulations performed in Ref. [4], at the pressure of 40 bar and the initial kinetic energy of muonic hydrogen of about 20 eV, the thermalization time is about 150 ns. The typical time of the spin flip is an order of magnitude less (10–15 ns). Thus, after thermalizing almost all muonic atoms are in the lower state of the hyperfine structure. If now a laser pulse passes through the gas, a part of muonic atoms will be found in an upper state with $F = 1$. Colliding with hydrogen molecules, these atoms go back to the state with $F = 0$. In each such collision, the transition energy of 0.18 eV is divided between the muonic atom and the hydrogen molecule. Taking into account their mass ratio and rotational transitions in the molecule, it is possible to assert that the muonic atom gets an additional kinetic energy of about 0.1 eV. Thus, after passing the laser pulse, the gas contains both thermalized and epithermal muonic atoms in the state with $F = 0$. It is obvious that the dependence of the number of epithermal muonic atoms on the laser radiation frequency has a resonant character. If the shape of this dependence is known from an experiment, the hyperfine splitting energy can be determined. If the muon transfer reaction to a heavier nucleus is used to record epithermal muonic atoms, the transfer from thermalized muonic atoms is an unwanted background. The most suitable reaction is the one whose rate increases sharply as the collision energy changes from thermal to epithermal values. The muon transfer to oxygen satisfies this requirement. In this case, the observable quantity is the number of delayed X-ray quanta emitted by muonic atoms of oxygen. Since this number is proportional to the amount of the muonic atoms, it should also depend resonantly on the laser radiation frequency.

In order to choose optimal conditions for the laser experiment, new measurements of the rate of the reaction (1) were performed in Refs. [5, 6]. The authors set a goal to determine the energy dependence of the reaction rate at thermal and epithermal energies. In order to avoid uncertainties related to the initial energy distribution of muonic hydrogen atoms, the muon transfer from thermalized muonic atoms was observed, and the temperature dependence of the rate $\lambda(T)$ was studied. The gaseous hydrogen–oxygen mixture used in this experiment was under the pressure of 41 bar, the oxygen concentration was equal to 190 ppm, and the temperature varied from 104 to 300 K. Similarly to Ref. [2], time spectra of X-ray quanta radiated by muonic atoms of oxygen were observed. The transfer rate was determined from the slope of the part of these spectra that is more than one microsecond apart from the instant of formation of muonic oxygen atoms. The obtained results are presented in Table 1. They were first published in Ref. [5] and then, after some corrections, in Ref. [6]. The new values of the transfer rate obtained at room temperature agree well with the result (3). One should pay attention to the fast growth of the transfer rate with temperature. This fact means that the $1/v$ law for the reaction cross section is not valid at collision energies corresponding to the temperatures considered. In order to reproduce the temperature dependence obtained in the experiment, the authors of Ref. [5] proposed a simple polynomial approximation of the energy dependence of the transfer rate, which, in the authors' opinion, is

valid in the collision–energy interval of 0.01 – 0.1 eV:

$$q(E) = p_1 + p_2 E + p_3 E^2. \quad (4)$$

The values of the coefficients p_i are given in Table 2. They were obtained by averaging the function (4) over the Maxwellian distribution and fitting the result to the experimental data presented in Table 1. If the central values of the coefficients are taken, the maximum of the function (4) is reached at the energy of 0.097 eV. The maximum value of the transfer rate is $1.74 \times 10^{11} \text{ s}^{-1}$, and it agrees qualitatively with the result (3) for epithermal energies. Measurements of the transfer rate $\lambda(T)$ were recently extended towards lower and higher temperatures [7]. The obtained results are also given in Table 1. It is seen that the transfer rate slowly decreases at $T \leq 104 \text{ K}$. This corresponds to the statement that the transfer rate becomes temperature independent at low T . At $T > 300 \text{ K}$, the transfer rate continues to increase.

Table 1: Experimental values of the rate $\lambda(T)$ of the muon transfer from thermalized muonic hydrogen atoms to oxygen at various temperatures. The errors are given in the form $\pm \sigma_1 \pm \sigma_2$, where σ_1 includes statistical and systematic errors related to the background subtraction from X-ray energy spectra, and σ_2 represents other systematic errors. The value marked by an asterisk was measured in the interval of 60 – 79 K, and it was attributed to the temperature of 70 K.

$T, \text{ K}$	$\lambda(T), 10^{10} \text{ s}^{-1}$		
	[5]	[6]	[7]
70	—	—	* $2.67 \pm 0.40 \pm 0.32$
80	—	—	$2.96 \pm 0.11 \pm 0.36$
104	$3.25 \pm 0.10 \pm 0.07$	$3.07 \pm 0.29 \pm 0.07$	—
153	$5.00 \pm 0.11 \pm 0.10$	$5.20 \pm 0.33 \pm 0.10$	—
201	$6.38 \pm 0.10 \pm 0.13$	$6.48 \pm 0.32 \pm 0.13$	—
240	$7.62 \pm 0.12 \pm 0.16$	$8.03 \pm 0.35 \pm 0.16$	—
272	$8.05 \pm 0.12 \pm 0.17$	$8.18 \pm 0.37 \pm 0.17$	—
300	$8.68 \pm 0.12 \pm 0.18$	$8.79 \pm 0.39 \pm 0.18$	—
323	—	—	$8.88 \pm 0.62 \pm 0.66$
336	—	—	$9.37 \pm 0.57 \pm 0.70$

Table 2: Coefficients of the quadratic trinomial (4) approximating the energy dependence of the muon transsfer rate in the collision–energy interval of 0.01 – 0.1 eV [5].

$p_1, \text{ s}^{-1}$	$p_2, \text{ s}^{-1} \text{ eV}^{-1}$	$p_3, \text{ s}^{-1} \text{ eV}^{-2}$
$(-1.32 \pm 0.61) \times 10^{10}$	$(3.85 \pm 0.54) \times 10^{12}$	$(-1.98 \pm 0.65) \times 10^{13}$

Table 3: Experimental λ_{exp} and theoretical λ_{th} values of the rate $\lambda(T)$ of the muon transfer from thermalized muonic hydrogen atoms to oxygen at room temperature. All the rates are given in units of 10^{10} s^{-1} . The rate obtained in Ref. [8] was reduced to the density $N_{\text{H}} = 4.25 \times 10^{22} \text{ cm}^{-3}$. The value from Ref. [9] is the rate $q(E)$ at the mean thermal energy of 0.04 eV. The other rates were obtained by averaging over the Maxwellian distribution. Two values from Ref. [13] correspond to the muon transfer to a bare oxygen nucleus (the upper value) and to the nucleus of a free atom with allowance for the electron screening (the lower value).

λ_{exp} [2]	λ_{th}				
	[8]	[9]	[10]	[11, 12]	[13]
8.5 ± 0.2	6.8	7.7 ± 0.5	8.4	7.77	23.2
					4.42

Let us now consider results of available calculations of the muon transfer rate [8–13]. It should be noted that in the reaction (1) the muon is transferred to a nucleus of the oxygen molecule. In the calculations performed to date, molecular effects were not taken into account, although they may be significant at low collision energies. The calculations were performed for the muon transfer either to a bare nucleus with no electron shell or to the nucleus of a free atom. In the latter case, the screening of the nuclear charge by atomic electrons was considered in the polarization interaction between muonic hydrogen and oxygen. The transfer rates calculated for muonic hydrogen atoms thermalized at room temperature are presented in Table 3. All of them, with the exception of the results of Ref. [13], are in reasonable agreement with experimental data. The situation with the energy dependence of the transfer rate is more complicated. In Ref. [8], the muon transfer to a bare oxygen nucleus was considered within the Landau–Zener model. In taking into account only the s -wave contribution, it was found that, as the collision energy increases, the transfer rate was initially constant and then began to decrease. A similar dependence was obtained in Ref. [9]. The respective calculation was performed on the basis of Faddeev equations for collision energies below 0.5 eV. As well as in Ref. [8], the muon transfer to a bare oxygen nucleus was considered, and only the s -wave contribution was taken into account. An important step was made in Ref. [10]. The authors considered contributions of partial waves with nonzero values of the orbital angular momentum. They used the two-state approximation and the Landau–Zener model in a more refined version than in Ref. [8]. Moreover, the electron screening in the entrance channel of the transfer reaction was taken into account. As a result, the existence of a d -wave resonance in the transfer rate was predicted at collision energies of about 0.19 eV. The resonance width and the peak value of the transfer rate agree qualitatively with the experimental result (3) for epithermal energies. Subsequently, the role of partial waves with nonzero orbital angular momenta was studied in Refs. [11, 12]. The calculation of the transfer rate was performed within the method of hyperspherical elliptic coordinates; the electron screening was not considered. The results of this calculation differ drastically from the ones of Ref. [10]. It was obtained that, in the energy interval between 2×10^{-3} and 1 eV, the p -wave made the main contribution to the muon transfer

rate. As the collision energy increases, the rate passes through a broad maximum at thermal energies, reaching a value of about $8 \times 10^{10} \text{ s}^{-1}$, and then it decreases monotonically up to the energy of 2 eV. Thus, the calculation performed in Refs. [11, 12] correctly reproduces the value of the transfer rate from thermalized muonic atoms, but its results contradict the experimental fact of the increase of the transfer rate at epithermal energies. At last, one more calculation was performed in Ref. [13]. The authors used a version of the hyperspherical functions method and considered the muon transfer both to a bare oxygen nucleus and to the nucleus of a free atom with allowance for the electron screening. In both the cases, a broad p -wave maximum in the energy dependence of the transfer rate was predicted, but its position and height proved to be very sensitive to the electron screening. In the case of the transfer to a bare nucleus, the maximum was also located at thermal energies, but its height was about eight times larger than that obtained in Refs. [11, 12]. In taking into account the electron screening, the curve of the energy dependence went down strongly at energies below 0.1 eV. As a result, the maximum shifted to the energy of 0.11 eV and became less sharp. The maximum value of the transfer rate was obtained to be nearly equal to $1.3 \times 10^{11} \text{ s}^{-1}$. This result agrees qualitatively with the observed increase of the transfer rate at epithermal energies. Concerning the transfer rate from thermalized muonic atoms, the calculation did not reproduce its experimental value closely. The rate obtained for the transfer to a bare nucleus was about three times large. In this case, the electron screening proved to be even more significant. It reduced the transfer rate nearly by a factor of six down to a half of the experimental value. Thus, the results of the calculations performed in Refs. [10–13] show the importance of taking into account partial waves with nonzero orbital angular momenta and the electron screening. However, the energy dependences of the transfer rate predicted in these studies are substantially different.

In connection with the ambiguity of the theoretical results considered above, in the present study, the rate of the reaction (1) was calculated for collision energies from 10^{-4} to 10 eV. A version of the perturbed stationary states method was used. It was proposed in Ref. [14] and applied to calculations of the muon transfer rate from hydrogen to neon in Ref. [15]. This method is based on a substantial difference of the energies of relative motion in the reaction channels. The reaction of the muon transfer to oxygen satisfies this condition. The analysis of energy spectra of delayed X-ray quanta performed in Ref. [2] showed that, in the reaction (1), muons were transferred to muonic oxygen states with the principle quantum number $n \leq 6$. In this case, the kinetic energy of relative motion of the reaction products is at least 2.4 keV, and it is much greater than the above-mentioned collision energies in the entrance channel. It is obvious that, in this case, it is first of all necessary to provide an asymptotically correct description of the entrance channel. Therefore, the wave function of the three-body system (muon, proton, and oxygen nucleus) was constructed in the form of an expansion in eigenfunctions of a two-center Coulomb problem formulated in terms of the Jacobi coordinates of the entrance channel. Since this method was described in detail in Ref. [14], only its brief overview is given in Sec. 2. Some details of the calculation are discussed in Sec. 3. The results and conclusions are presented in Sec. 4. Unless otherwise stated, the muon-atom units

will henceforth be used:

$$\hbar = e = m_\mu = 1, \quad (5)$$

e is the proton charge, m_μ is the muon mass; the unit of length is 2.56×10^{-11} cm, and the unit of energy is 5.63 keV.

2. METHOD OF CALCULATIONS

The reaction of the direct muon transfer to oxygen is a particular case of the charge-exchange reaction in a collision between a muonic atom of a hydrogen isotope H in the $1s$ state and a nucleus of an atomic number $Z > 1$:

$$\mu\text{H}(1s) + Z \rightarrow \mu Z^* + \text{H}, \quad (6)$$

where μZ^* is a muonic atom of the element Z in an excited state. Let us introduce the Jacobi coordinates of the entrance channel of this reaction: the vector \mathbf{r} specifying the muon position with respect to the hydrogen nucleus and the vector \mathbf{R} connecting the center of mass C_2 of the muonic hydrogen atom with the Z nucleus (Fig. 1). The center of mass C_3 of the three-body system lies on the vector \mathbf{R} . Let us introduce a few more quantities: the vector \mathbf{r}_1 drawn from the point C_2 to the muon, the distance r_2 between the muon and the Z nucleus, and the distance R_{HZ} between the nuclei. The nonrelativistic three-body Hamiltonian written in the center-of-mass frame is:

$$\hat{H} = -\frac{1}{2M} \Delta_{\mathbf{R}} + \hat{H}_\mu + \frac{Z}{R_{\text{HZ}}}. \quad (7)$$

The first term is the kinetic-energy operator of the relative motion of the muonic hydrogen atom and the Z nucleus, M is the reduced mass of the Z nucleus with respect to the muonic atom:

$$M^{-1} = (M_{\text{H}} + 1)^{-1} + M_Z^{-1}, \quad (8)$$

where M_{H} and M_Z are the nuclear masses. The term \hat{H}_μ is the Hamiltonian of the muonic hydrogen atom supplemented with the potential energy of the Coulomb interaction of the muon and the Z nucleus:

$$\hat{H}_\mu = -\frac{1}{2m_{\mu\text{H}}} \Delta_{\mathbf{r}} - \frac{1}{r} - \frac{Z}{r_2}, \quad (9)$$

where $m_{\mu\text{H}}$ is the reduced mass of the muonic hydrogen atom:

$$m_{\mu\text{H}}^{-1} = M_{\text{H}}^{-1} + 1. \quad (10)$$

The last term in (7) describes the Coulomb repulsion of the H and Z nuclei.

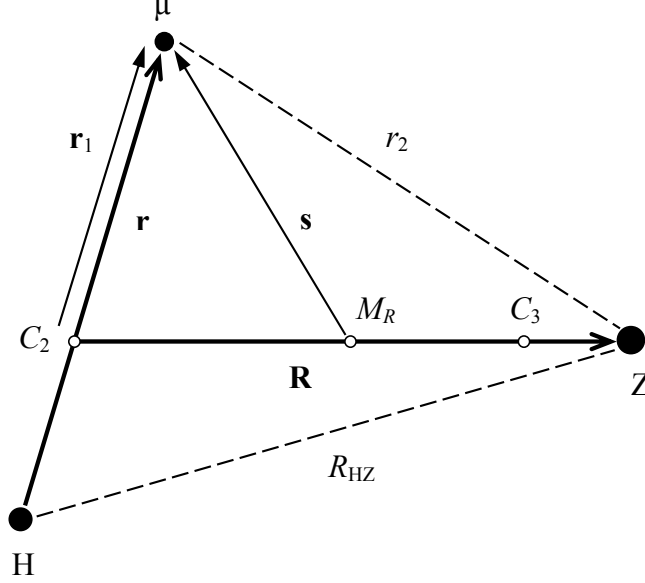


Figure 1: Jacobi coordinates of the entrance channel of the muon transfer reaction. C_2 is the center of mass of the muonic hydrogen atom, C_3 is the center of mass of the three-body system, M_R is the midpoint of the vector \mathbf{R} .

Let us single out a two-center problem in the three-body Hamiltonian. For this purpose, let us rewrite the term \hat{H}_μ as follows [16]:

$$\hat{H}_\mu = m_{\mu\text{H}} \cdot \hat{h}_\mu, \quad (11)$$

$$\hat{h}_\mu = -\frac{1}{2} \Delta_{\mathbf{s}} - \frac{1}{r_1} - \frac{Z'}{r_2}. \quad (12)$$

The vector \mathbf{s} connects the midpoint M_R of the vector \mathbf{R} with the muon:

$$\mathbf{s} = \mathbf{r}_1 - \frac{\mathbf{R}}{2}, \quad \mathbf{r}_1 = m_{\mu\text{H}} \cdot \mathbf{r}. \quad (13)$$

The charge Z' is:

$$Z' = \frac{Z}{m_{\mu\text{H}}}. \quad (14)$$

The operator \hat{h}_μ is the Hamiltonian of a muon in the field of two immovable Coulomb centers whose charges are equal to unity and Z' . The unit charge is placed in the center of mass of the muonic hydrogen atom, while the position of the charge Z' coincides with the one of the Z nucleus. For the muon transfer from protium to oxygen, the charge Z' is:

$$m_{\mu\text{H}} = 0.899, \quad Z' = 8.90. \quad (15)$$

In the coordinate frame with the origin in the point M_R and the polar axis directed along the vector \mathbf{R} , the muon position is specified by the prolate spheroidal coordinates ξ , η , and φ [17]:

$$\xi = \frac{r_1 + r_2}{R}, \quad \eta = \frac{r_1 - r_2}{R}. \quad (16)$$

The azimuthal angle φ lies in the plane that is orthogonal to vector \mathbf{R} and which contains the point M_R . Surfaces of constant values of the coordinates ξ and η are respectively prolate ellipsoids of revolution and two-sheeted hyperboloids. These surfaces have the foci at the points C_2 and Z for which $\xi = 1$ and $\eta = \mp 1$.

Let us consider the eigenvalue problem for the two-center Hamiltonian \hat{h}_μ :

$$\hat{h}_\mu \psi_{jm}(\xi, \eta; R) \frac{\exp(\pm im\varphi)}{\sqrt{2\pi}} = \varepsilon_{jm}(R) \psi_{jm}(\xi, \eta; R) \frac{\exp(\pm im\varphi)}{\sqrt{2\pi}}. \quad (17)$$

Here the dependence on the angle φ is explicitly singled out, the quantum number m takes non-negative integer values, and the index j stands for the set of the remaining quantum numbers. For bound states, these are either the numbers n_ξ and n_η of nodes in the respective variables or the parabolic quantum numbers n_1 and n_2 in the limit of $R \rightarrow \infty$ [17]. The two-center problem (17) is solved at a fixed distance R , which appears in eigenfunctions and eigenvalues $\varepsilon_{jm}(R)$ as a parameter. The functions $\psi_{jm}(\xi, \eta; R)$ can be chosen to be real-valued. The eigenfunctions with identical m and different sets i and j of the remaining quantum numbers are orthonormalized:

$$\int \psi_{im}(\xi, \eta; R) \psi_{jm}(\xi, \eta; R) d\tau = \delta_{ij}, \quad (18)$$

$$d\tau = (R/2)^3 (\xi^2 - \eta^2) d\xi d\eta. \quad (19)$$

Here the integral is taken over the region specified by the inequalities $1 \leq \xi < \infty$ and $-1 \leq \eta \leq +1$. The orthonormality in m is ensured by the factors $\exp(\pm im\varphi)/\sqrt{2\pi}$. It is obvious that the solutions of the problem (17) are also the eigenfunctions of the Hamiltonian \hat{H}_μ with the eigenvalues $m_{\mu H} \cdot \varepsilon_{jm}(R)$.

It is well known that the two-center problem admits the separation of variables in prolate spheroidal coordinates [17]. The function $\psi_{jm}(\xi, \eta; R)$ is the product of a radial and an angular function. The former depends only on ξ , while the latter depends only on η . By solving two differential equations for these functions with respective boundary conditions, one can find the eigenvalue $\varepsilon_{jm}(R)$, the separation constant, and eventually construct the eigenfunction. In the previous calculation of the muon transfer rate to neon [15], this scheme was implemented on the basis of standard expansions of the radial and angular functions in infinite series [18–20]. The eigenvalue $\varepsilon_{jm}(R)$ and the separation constant were determined on the basis of the method proposed in Ref. [21] and modified for the case in which the expansion coefficients are not monotonic functions of their number. This scheme was also used in the present study.

The primary coordinate frame in which the motion of three particles is considered has fixed axes and the origin at the center of mass C_3 . The Hamiltonian \hat{H} commutes with the operator $\hat{\mathbf{J}}^2$ of the square of the orbital angular momentum of the three-body system and with the operator \hat{J}_z of its projection onto the z -axis of the primary coordinate frame. In addition, \hat{H} commutes with the operator \hat{P} of inversion of the spatial coordinates of all the particles. It is convenient to take the eigenfunctions of these three operators as basis solutions in which the three-body wavefunction is expanded. Let us also require them to be solutions of the two-center problem (17). Since, in

this problem, the muon coordinates are associated with the vector \mathbf{R} , let us introduce the polar and azimuthal angles Θ and Φ specifying the orientation of \mathbf{R} with respect to the axes of the primary coordinate frame. Then a configuration of the three-body system is specified by the six independent coordinates R , Θ , Φ , ξ , η , and φ , and the basis solutions are:

$$\Psi_{Mjm}^{JP}(R, \Theta, \Phi, \xi, \eta, \varphi) = \frac{\chi_{jm}^{JP}(R)}{R} \Upsilon_{Mm}^{JP}(\Phi, \Theta, \varphi) \psi_{jm}(\xi, \eta; R). \quad (20)$$

Here $\chi_{jm}^{JP}(R)$ is a radial function that depends on the quantum numbers indicated in the indices, $\Upsilon_{Mm}^{JP}(\Phi, \Theta, \varphi)$ is the eigenfunction of the operators $\hat{\mathbf{J}}^2$, \hat{J}_z , and \hat{P} for the eigenvalues $J(J+1)$, M , and P . The nonnegative integer m introduced in Eq. (17) is the modulus of the projection of the total orbital angular momentum of the three-body system onto the direction of the vector \mathbf{R} . The functions Υ_{Mm}^{JP} are orthonormalized:

$$\int_0^\pi \sin \Theta d\Theta \int_0^{2\pi} d\Phi \int_0^{2\pi} d\varphi (\Upsilon_{Mm}^{JP})^* \Upsilon_{M'm'}^{JP} = \delta_{JJ'} \delta_{PP'} \delta_{MM'} \delta_{mm'}. \quad (21)$$

Their specific form depends on m . If $m = 0$, then

$$\Upsilon_{Mm=0}^{JP}(\Phi, \Theta, \varphi) = \frac{Y_{JM}(\Theta, \Phi)}{\sqrt{2\pi}}, \quad (22)$$

where $Y_{JM}(\Theta, \Phi)$ is the spherical harmonic. In this case, the parity is unambiguously determined by the quantum number J : $P = (-1)^J$. If $m \neq 0$, then

$$\Upsilon_{Mm}^{JP}(\Phi, \Theta, \varphi) = \frac{\sqrt{2J+1}}{4\pi} \left[(-1)^m D_{Mm}^J(\Phi, \Theta, \varphi) + P (-1)^J D_{M(-m)}^J(\Phi, \Theta, \varphi) \right], \quad (23)$$

where D_{Mm}^J and $D_{M(-m)}^J$ are the Wigner functions [22] transformed under the inversion as follows:

$$D_{Mm}^J(\Phi, \Theta, \varphi) \longrightarrow (-1)^{J-m} D_{M(-m)}^J(\Phi, \Theta, \varphi). \quad (24)$$

In this case, two parity values are possible at given J : $P = \pm(-1)^J$.

Let us consider the time-independent Schrödinger equation for the three-body wavefunction with the quantum numbers J , M , and P :

$$\hat{H} \Psi_M^{JP} = \tilde{E} \Psi_M^{JP}. \quad (25)$$

For the reaction (6), the energy of the system \tilde{E} is:

$$\tilde{E} = E_{\mu\text{H}}(1s) + E, \quad (26)$$

where $E_{\mu\text{H}}(1s)$ is the ground-state energy of the muonic hydrogen atom:

$$E_{\mu\text{H}}(1s) = -\frac{m_{\mu\text{H}}}{2}, \quad (27)$$

and E is the collision energy:

$$E = \frac{Mv^2}{2} = \frac{k^2}{2M}. \quad (28)$$

Here v is the velocity of the relative motion of the μH atom and the Z nucleus at infinite separation, and $k = Mv$ is the asymptotic momentum of the relative motion.

Let us seek a solution of Eq. (25) in the form of an expansion in the basis solutions (20):

$$\Psi_M^{JP} = \sum_{jm} \Psi_{Mjm}^{JP}. \quad (29)$$

The substitution of this expansion into Eq. (25) and the integration over the variables Θ, Φ, ξ, η , and φ with allowance for the orthonormality of the basis solutions lead to a set of coupled second-order differential equations for the radial functions $\chi_{jm}^{JP}(R)$. These equations were presented in Ref. [14]. In practice, the contribution of a finite number of two-center states is taken into account in the expansion (29). After solving the obtained set of equations with respective boundary conditions, one can calculate the total cross section of the reaction (6).

As already noted, the main idea of the method under discussion consists in constructing an asymptotically correct description of the entrance reaction channel at large values of the distance R . In the limit of $R \rightarrow \infty$, the solutions of the two-center problem (17) split into two groups. The states of one group are localized near the left center, which is placed in the center of mass of the μH atom and carries the unit charge. The states of the other group are localized near the right center Z' . The simplest way to describe the entrance channel is to take into account the only state of the left-center group. Its asymptotic quantum numbers are:

$$m = n_1 = n_2 = 0, \quad n = 1, \quad (30)$$

where n_1 and n_2 are the parabolic quantum numbers, and $n = n_1 + n_2 + m + 1$ is the principle quantum number. Hereinafter all the quantities related to this state will be marked with the index 0. In the limit considered, the eigenfunction ψ_0 and the eigenvalue $\varepsilon_0(R)$ of the two-center problem are:

$$\psi_0 \propto \exp(-m_{\mu\text{H}} \cdot r), \quad \varepsilon_0(R \rightarrow \infty) = -\frac{1}{2}. \quad (31)$$

Thus, the two-center eigenfunction goes into the wave function of the ground state of the μH atom with the correct value of the reduced mass. This is because the left center lies at the center of mass of the muonic hydrogen atom; the argument of the exponent in the function ψ_0 is the distance from this center to the muon. The eigenvalue of the Hamiltonian \hat{H}_μ tends to the correct dissociation limit:

$$m_{\mu\text{H}} \cdot \varepsilon_0(R \rightarrow \infty) = E_{\mu\text{H}}(1s). \quad (32)$$

At large R , the relative motion in the entrance channel is determined by the potential $U_0(R)$, which is obtained by averaging the three-body Hamiltonian over the state ψ_0 . The expansion of this potential in powers of R^{-1} was considered in Ref. [14]. The leading term of this expansion is proportional to R^{-4} and corresponds to the polarization attraction between the muonic hydrogen atom and the Z nucleus:

$$U_0(R) = -\frac{\beta_0 Z^2}{2R^4}. \quad (33)$$

The polarizability of the muonic atom was found to be:

$$\beta_0 = \beta \left[1 - \frac{1}{(M_H + 1)^2} \right], \quad (34)$$

where β is the exact value of the polarizability:

$$\beta = \frac{9}{2m_{\mu H}^3}. \quad (35)$$

It should be noted that, because of the cube of the reduced mass in the denominator of this expression, the value of β can differ markedly from the frequently used value of 4.5, which corresponds to an infinitely heavy nucleus H. In particular, $\beta \approx 6.2$ for muonic protium. Although β_0 does not coincide with β , their values are very close. For muonic protium, $\beta_0 \approx 0.99\beta$. The distinction between these values is due to the fact that the Coulomb repulsion of the nuclei (the last term in Eq. (7)) is not diagonal in the two-center basis. As was shown in Ref. [14], taking this circumstance into account leads to a small correction to the polarizability. Its addition to β_0 yields β exactly. Thus, the use of only one state of the left center already provides a good description of the entrance reaction channel at large R : the dissociation limit is correct, no spurious long-range interactions appear (at least to terms of order R^{-4} inclusive), and the polarizability of the muonic hydrogen atom is reproduced to within 1 %. Therefore, this description will be used in the following. Moreover, since the values of β and β_0 are close, the polarization potential with the exact value of β will be used to describe the relative motion in the entrance channel at large R :

$$U_p(R) = -\frac{\beta Z^2}{2R^4}. \quad (36)$$

Within the approach considered, the muon transfer channel is described by states of the right center. In the limit of $R \rightarrow \infty$, they correspond to the $\mu Z'$ atom with an infinitely heavy nucleus rather than to the real μZ atom. In particular, the wave functions of these states do not contain the reduced mass of the μZ atom at all. Moreover, the equations for the radial functions of the relative motion in the transfer channel remain coupled even at an infinitely large distance R . The reason of these difficulties is the use of the entrance-channel Jacobi coordinates, which are not natural for the transfer channel. It is obvious that, in this case, it is impossible to calculate cross sections of the muon transfer to individual states of the μZ atom. Nevertheless, since the states of the right center are asymptotically localized near the Z nucleus, a group of these states as a whole describes the migration of the muon charge cloud from H to Z , i.e. the muon transfer. Therefore, it is possible to calculate the total transfer cross section. This calculation is based on the fact that, at large R , the basis two-center functions describing the entrance and transfer channels are localized at the different centers. Therefore, as R increases, the matrix elements of the three-body Hamiltonian that couple the equations for the radial functions of these channels decrease exponentially. As a result, at $R \rightarrow \infty$, the set of radial equations splits into two groups, which describe the channels separately. In the simplest approximation in which the only left-center state with the quantum numbers (30) is taken into account, the entrance channel is asymptotically

described by one equation:

$$\frac{d^2 \chi_0^J}{dR^2} + \left[k^2 - \frac{J(J+1)}{R^2} - 2MU_p(R) \right] \chi_0^J = 0, \quad (37)$$

where χ_0^J is the radial function of the entrance channel. Its upper index P is omitted because at $m = 0$ the parity is unambiguously determined by the quantum number J : $P = (-1)^J$. The boundary condition for this function at large R is:

$$\chi_0^J(R \rightarrow \infty) \longrightarrow \sin(kR - J\pi/2) + Q_0^J \exp[i(kR - J\pi/2)]. \quad (38)$$

The complex amplitude Q_0^J depends on J and k . The radial functions of the transfer channel behave asymptotically as divergent waves. A method of constructing such solutions for coupled equations was described in Ref. [14]. The boundary condition at $R = 0$ is standard: the radial functions vanish at this point.

By integrating the set of coupled radial equations under the above boundary conditions, it is possible to construct the amplitudes Q_0^J . Let us rewrite the asymptotic radial function χ_0^J in the following form:

$$\chi_0^J(R \rightarrow \infty) \propto \exp[-i(kR - J\pi/2)] - S_0^J \exp[i(kR - J\pi/2)], \quad (39)$$

where S_0^J is the diagonal S -matrix element corresponding to the entrance channel:

$$S_0^J = 1 + 2iQ_0^J. \quad (40)$$

Since the muon transfer is the only inelastic channel at the collision energies considered, the total cross section of the muon transfer is [22]:

$$\sigma(E) = \frac{\pi}{k^2} \sum_{J=0}^{\infty} (2J+1) \left(1 - |S_0^J|^2 \right). \quad (41)$$

The muon transfer rate $q(E)$ considered as a function of the collision energy and normalized to the atomic density of liquid hydrogen is calculated by the formula (2). The rate $\lambda(T)$ of the muon transfer from thermalized muonic hydrogen atoms is obtained by averaging the rate $q(E)$ over the Maxwellian distribution of relative velocities in the entrance channel.

3. SOME DETAILS OF THE CALCULATION

Let us consider how the method described in Sec. 2 is applied to the calculation of the rate of the muon transfer from hydrogen to oxygen. At large interatomic distances, the entrance reaction channel is described by one left-center state ψ_0 with the quantum numbers (30). In order to choose the relevant right-center states, let us take advantage of the generally accepted viewpoint that the muon transfer from hydrogen to a heavier nucleus is mainly due to quasicrossings of adiabatic terms associated with the reaction channels. The right-center states will be specified by the parabolic

quantum numbers n'_1 and n'_2 , and by the principle quantum number $n' = n'_1 + n'_2 + m + 1$. As is known [17], quasicrossings are possible only for terms with identical values of the numbers m and n_1 . Since these numbers are equal to zero for the state ψ_0 , let us consider right-center states with $m = n'_1 = 0$. Their wave functions have no nodes in the variable ξ but differ in the number n_η of nodes in the variable η . In the following, the states with $3 \leq n'_2 \leq 6$ will be of interest. According to the relation between n_η and n'_2 [17], $n_\eta = n'_2$ for these states at $Z' = 8.90$. The dependences of the eigenvalues ε_j of the two-center problem (17) on the interatomic distance R are shown in Fig. 2 (the index j is now reduced to the numbers n'_1 and n'_2). Quasicrossings occur in the following regions of R : 4–6, 7–8, and 12–13. If we begin from the $n'_2 = 3$ term and move toward large R , then each transition from one term to another in a quasicrossing region increases n'_2 by unity. This corresponds to the general rule [17] that the terms involved into a quasicrossing differ in n_η by unity. There are two more quasicrossings not shown in Fig. 2. One of them lies at $R \approx 24.3$. For it, the number n'_2 increases from 6 to 7. Finally, the farthest quasicrossing lies at $R \approx 66$. It involves the right-center state with $n'_2 = 7$ and the state ψ_0 for which the number of nodes $n_\eta = 8$.

Let us assume that the muonic hydrogen atom is at a very large distance R from the oxygen nucleus. In this case, the function ψ_0 is localized in a vicinity of the proton, where it coincides nearly with the wave function of the ground state of an isolated muonic hydrogen atom. All eight nodes of this function lie in a vicinity of the oxygen nucleus, where ψ_0 is exponentially small. As R decreases, this pattern remains unchanged up to the first quasicrossing with the right-center state with $n'_2 = 7$. After passing through the quasicrossing region, the muon charge distribution in these states changes abruptly. In the ψ_0 state, the muon charge cloud migrates to the oxygen nucleus and becomes exponentially small near the proton. In the $n'_2 = 7$ state, the charge, on the contrary, flows to the proton, and all seven nodes of the wave function prove to be in a vicinity of the oxygen nucleus, where the wave function is exponentially small. A similar picture is observed in passing through other quasicrossings, which occur deep under the potential barrier separating the Coulomb wells of the two-center problem. In this case, it can be argued that, between narrow quasicrossing regions, the muon charge cloud is localized near one of the Coulomb centers and, as R decreases, the right-center states with the number n'_2 successively decreasing by unity describe the muonic hydrogen atom in the Coulomb field of the oxygen nucleus. In particular, this is the $n'_2 = 6$ state in the region of $13 < R < 24$. The fact that it does correspond to the muonic hydrogen atom in the field of the oxygen nucleus is confirmed by calculations of the adiabatic potential that is equal to the sum of the eigenvalue $m_{\mu\text{H}} \cdot \varepsilon_j(R)$ of the Hamiltonian \hat{H}_μ counted from the energy $E_{\mu\text{H}}(1s)$ of the isolated muonic hydrogen atom and the average value of the Coulomb repulsion of the nuclei. At $R = 24$, this potential agrees with the polarization potential with two percent accuracy. As R decreases further, the quasicrossings occur closer and closer to the barrier top, the quasicrossing regions become broader, and the statement that the muon is localized near one of the nuclei loses meaning. In our case, the quasicrossings at $R = 4 - 6$ and $7 - 8$ occur near the barrier top.

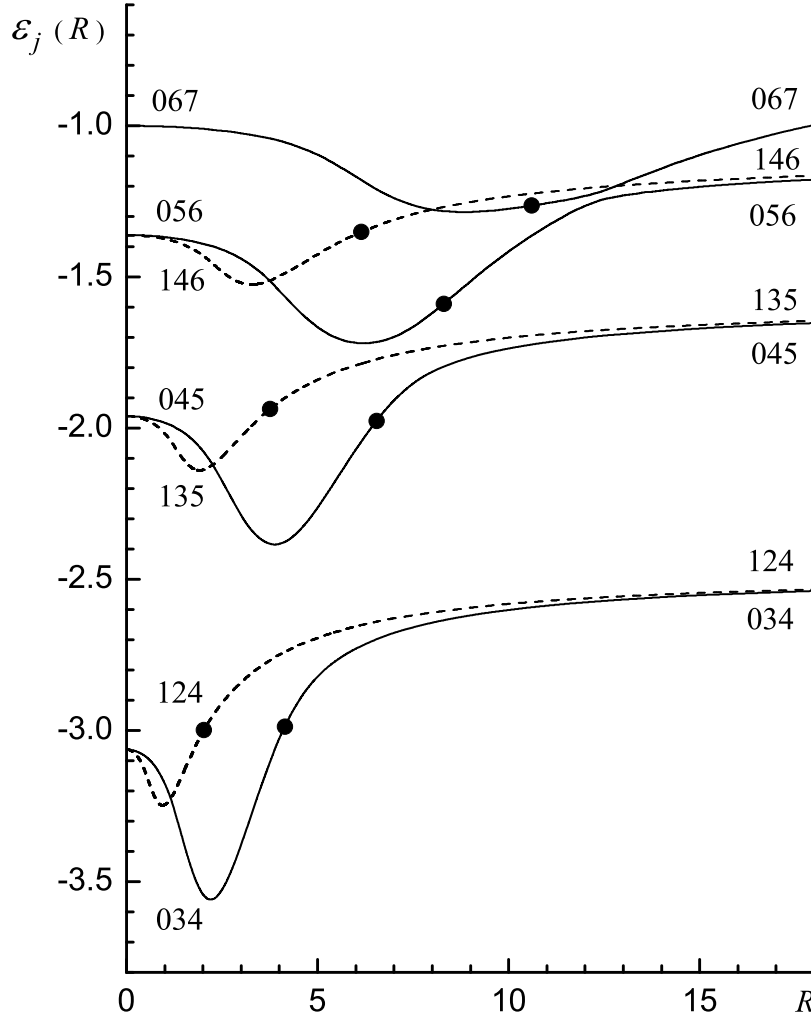


Figure 2: Eigenvalues $\varepsilon_j(R)$ of the two-center Coulomb problem versus the interatomic distance R for some right-center states with $m = 0$. All the values are given in muon-atom units. Each curve is marked with the values of the parabolic quantum numbers n'_1 , n'_2 , and n' . The solid and dashed curves correspond respectively to states with $n'_1 = 0$ and 1. The black circle on each curve indicates the value of R at which the respective state crosses the top of the potential barrier separating the Coulomb wells of the two-center problem.

According to the generally accepted viewpoint, the muon transfer is due to not too distant quasicrossings occurring near the barrier top. For example, in Refs. [8, 10], the muon transfer to oxygen was considered on the basis of an analysis of terms of the two-center Coulomb problem with the charges of 1 and 8. It was found that the main contribution to the transfer rate came from quasicrossings for which the distance between the Coulomb centers lies in the interval of 8–9. By following these ideas, four right-center states were taken into account in the expansion of the

three-body wave function. Their quantum numbers are $m = n'_1 = 0$ and $n'_2 = 3 - 6$. Moreover, according to Ref. [8], states with $m = 0$ and $n'_1 = 1$ can play some role. Therefore, three such states with the quantum number $n'_2 = 2 - 4$ were also included into the calculation. For these states, the dependences of the eigenvalues ε_j on the distance R are also shown in Fig. 2. Their two-center wave functions have one node in the variable ξ ; the number of nodes in the variable η is equal to n'_2 . Thus, the basis used was composed of seven right-center states with $m = 0$. For convenience, their quantum numbers are presented in Table 4.

Table 4: Parabolic quantum numbers n'_1 and n'_2 of the right-center states with $m = 0$ in the limit of $R \rightarrow \infty$. $n' = n'_1 + n'_2 + m + 1$ is the principle quantum number. In the region of $13 < R < 24$, the state marked by an asterisk describes the muonic hydrogen atom in the Coulomb field of the oxygen nucleus. At $R \approx 24$, it corresponds to the entrance reaction channel. The remaining states describe the transfer channel.

n'_1	n'_2	n'
*0	6	7
0	5	6
0	4	5
0	3	4
1	4	6
1	3	5
1	2	4

When using the above two-center basis, there is a set of seven coupled equations for radial functions in the region on the left of the quasicrossing at $R \approx 24.3$. In the region of $13 < R < 24$, the right-center state with the quantum numbers $m = n'_1 = 0$ and $n'_2 = 6$ describes the muonic hydrogen atom in the field of the oxygen nucleus. The matrix elements coupling the equation for the radial function of this state with the remaining equations decrease exponentially with increasing R . Therefore, at $R \approx 24$ this equation splits off from the others and corresponds to the entrance reaction channel. As already mentioned, the adiabatic potential in this equation agrees with the polarization potential with two percent accuracy. At $R \geq 24$, the equation (37) with the polarization potential $U_p(R)$ was used to describe the entrance channel, i.e. the deep subbarrier quasicrossings lying at $R \approx 24.3$ and 66 were ignored. In this region of R , the muon transfer channel was described by six radial equations for the remaining states presented in Table 4.

The above consideration corresponds to the muon transfer to a bare oxygen nucleus. In fact, the muonic hydrogen atom collides with a molecule. In view of the complexity of this process, let us consider a collision of the muonic atom with a free oxygen atom. Even in this simplified case, an analysis of dynamics of the electron shell in the collision is a complicated problem. Indeed, the energy released in the muon transfer reaction is a few keV, and it is more than sufficient for electron excitations. The simplest approximation is to ignore the excitations and to assume that the electron shell remains in the ground state during the collision. In this case, the role of the electron shell reduces to screening the Coulomb interaction between heavy particles in reaction

channels. It is natural to expect that, because of low collision energies, the screening is most significant in the entrance channel. In the present study, the electron screening was taken into account in Eq. (37), which describes the entrance channel at $R \geq 24$. Instead of the polarization potential $U_p(R)$, a new spherically symmetric potential $U_e(R)$ was used. It was constructed by the method proposed in Ref. [23]. This potential can be written as the sum of two terms:

$$U_e(R) = U_s(R) + U_f(R). \quad (42)$$

The first term is the screened polarization potential:

$$U_s(R) = -\frac{\beta Z_a^2(R)}{2R^4}, \quad Z_a(R) = Z - Z_e(R). \quad (43)$$

$Z_e(R)$ is the absolute value of the electron charge in a sphere of radius R with the center at the nucleus of the atom, $Z_a(R)$ is the total charge of the atom in this sphere. The second term is due to a finite size of the muonic hydrogen atom. It can be considered as a contact interaction of the muonic atom with the electron shell:

$$U_f(R) = \frac{2\pi}{3} < r_{\mu H}^2 > \rho_e(R), \quad (44)$$

where $< r_{\mu H}^2 >$ is the mean square of the ground-state charge radius of the muonic atom with respect to its center of mass:

$$< r_{\mu H}^2 > = -\frac{3}{m_{\mu H}} \left(1 - \frac{1}{M_H} \right). \quad (45)$$

The square of the charge radius is negative because it is mainly contributed by the negatively charged muon. The function $\rho_e(R)$ is the absolute value of the electron density at the distance R from the Z nucleus. It is normalized by the condition

$$4\pi \int_0^\infty \rho_e(R) R^2 dR = Z. \quad (46)$$

The values of the potentials $U_s(R)$ and $U_f(R)$ are presented in Table 5 for a number of interatomic distances. The electron density $\rho_e(R)$ and the charge $Z_e(R)$ were calculated with the aid of analytic one-electron wave functions obtained by the Hartree-Fock-Roothaan method [24]. Both the potentials $U_s(R)$ and $U_f(R)$ are attractive and decrease exponentially with increasing R . Since $U_s(R)$ is proportional to the square of the atomic charge $Z_a(R)$ and involves the additional factor R^{-4} , it decreases faster. As a result, this potential is significant only at distances R that do not exceed the electron Bohr radius (about 200 muon-atom units). For example, at $R = 24$ the potential $U_s = -2.92$ eV, and it is one order of magnitude greater than the term U_f . Since the electron K -shell of the oxygen atom has approximately the same radius, the screening in the potential U_s is already noticeable: the atomic charge $Z_a = 7.45$. At $R \approx 105$, the potentials U_s and U_f become equal each other, and their sum is about -8.5×10^{-3} eV. This value is of the order of thermal energies at a temperature of 100 K. At $R = 200$, the term U_s is about 9 % of the potential

U_f . In this case, $U_e = 1.69 \times 10^{-3}$ eV, and it corresponds to thermal energies at a temperature of 20 K. One more fact associated with the potential U_f should be noted. The electron screening weakens the polarization attraction, so that the inequality $|U_s| < |U_p|$ holds at all values of R . The addition of the term U_f leads to the new potential U_e becoming greater in absolute value than U_p at $R > 115$: $|U_e| > |U_p|$. Since U_e decreases exponentially, while U_p follows the power law $1/R^4$, the opposite inequality holds at $R > 600$. The potentials are already very small at this point. They are about -8×10^{-6} eV, which corresponds to a temperature of about 0.1 K.

Table 5: Atomic charge Z_a and potential energies of interaction between the muonic hydrogen atom and the oxygen atom versus the interatomic distance R . The values of R and Z_a are given in muon-atom units, the potential energies are given in eV. The orders of values are indicated parenthetically.

R	Z_a	U_p	U_s	U_f	U_e
24	7.45	-3.36	-2.92	-1.97 (-1)	-3.11
30	7.20	-1.38	-1.12	-1.26 (-1)	-1.24
40	6.82	-4.36 (-1)	-3.17 (-1)	-6.09 (-2)	-3.77 (-1)
50	6.50	-1.79 (-1)	-1.18 (-1)	-3.05 (-2)	-1.49 (-1)
75	5.99	-3.53 (-2)	-1.98 (-2)	-7.89 (-3)	-2.77 (-2)
100	5.61	-1.12 (-2)	-5.49 (-3)	-4.41 (-3)	-9.89 (-3)
125	5.17	-4.57 (-3)	-1.91 (-3)	-3.45 (-3)	-5.36 (-3)
150	4.65	-2.20 (-3)	-7.44 (-4)	-2.74 (-3)	-3.48 (-3)
175	4.08	-1.19 (-3)	-3.09 (-4)	-2.10 (-3)	-2.41 (-3)
200	3.50	-6.97 (-4)	-1.34 (-4)	-1.56 (-3)	-1.69 (-3)
250	2.47	-2.86 (-4)	-2.73 (-5)	-8.19 (-4)	-8.46 (-4)
300	1.67	-1.38 (-4)	-6.03 (-6)	-4.19 (-4)	-4.25 (-4)
400	0.715	-4.36 (-5)	-3.48 (-7)	-1.09 (-4)	-1.10 (-4)
500	0.291	-1.79 (-5)	-2.35 (-8)	-2.95 (-5)	-2.96 (-5)
600	0.115	-8.61 (-6)	-1.79 (-9)	-8.27 (-6)	-8.27 (-6)
700	0.0455	-4.65 (-6)	-1.50 (-10)	-2.40 (-6)	-2.40 (-6)

In order to clarify the role of the electron screening, the calculations of the reaction rate were performed for three versions A, B, and C. They differ in the potential in Eq. (37), which asymptotically describes the entrance channel.

- A) The electron screening was fully ignored. This corresponds to the muon transfer to a bare oxygen nucleus. In this case, the unscreened polarization potential $U_p(R)$ was used in Eq. (37).
- B) The potential $U_p(R)$ was replaced by the screened polarization potential $U_s(R)$, i.e. the screening of the nuclear charge by atomic electrons was taken into account. Such a way was also applied in Refs. [10, 13].
- C) The potential $U_e(R) = U_s(R) + U_f(R)$ was used in Eq. (37). In this case, the contact interaction of the muonic hydrogen atom with the electron shell of oxygen was added to the

screened polarization potential. The version C is the most realistic because it takes into account the effect of atomic electrons to a greater extent than the versions A and B.

In all the versions, the effective potential appearing in Eq. (37) features a barrier at nonzero values of the orbital angular momentum J . The position of the barrier top R_b and its height U_b are given in Table 6 for $J \leq 4$. At these values of J , the barrier top lies either in the region of $R \geq 24$, where the entrance channel is described by Eq. (37) alone, or near this region on the left from it. At low collision energies $E \ll U_b$, the barrier prevents the penetration of the respective partial wave into the term–interaction region, and the contribution of this wave to the muon transfer cross section is small. As the collision energy grows, the partial cross section of the muon transfer increases and at $E \sim U_b$ becomes commensurate with the contributions of waves with lower orbital angular momenta.

Table 6: Position R_b of the top of the potential barrier and its height U_b for several values of the orbital angular momentum J according to calculations in the versions A, B, and C. The values of R_b are given in muon–atom units, the values of U_b are given in eV.

Version of calculation	$J = 1$		$J = 2$		$J = 3$		$J = 4$	
	R_b	U_b	R_b	U_b	R_b	U_b	R_b	U_b
A	60.5	0.0832	34.9	0.749	24.7	3.00	19.1	8.32
B	51.4	0.126	32.4	0.943	23.8	3.43	18.7	9.07
C	55.9	0.102	33.5	0.841	24.1	3.24	18.8	8.77

4. RESULTS OF THE CALCULATION AND CONCLUSIONS

The results of the present calculation of the muon transfer rate $q(E)$ are given in Figs. 3 and 4, and also in Appendix A. At low collision energies, the s -wave contribution predominates, the transfer cross section is proportional to $1/v$, and the transfer rate is nearly constant. At $E > 0.01$ eV, the contribution of the p -wave grows fast and becomes decisive. As a result, pronounced resonance maxima arise on the curves of the dependence $q(E)$. Their position and the maximum transfer rate obtained within the versions A, B, and C are given in Table 7. The position and the shape of the maxima depend substantially on the electron screening. The sharpest maximum is obtained in the version A (the muon transfer to a bare oxygen nucleus). In this case, the maximum value of the transfer rate is reached at a collision energy which is somewhat less than the height of the potential barrier in the p -wave. In the version B, taking into account the electron screening in the polarization potential reduces the attraction in the entrance reaction channel. As a result, the maximum shifts toward higher energies, and its height decreases. In the most realistic version C, the additional attraction caused by the contact interaction of the muonic hydrogen atom with the electron shell of oxygen shifts the maximum back to lower energies and increases its height. In the versions B and C, the maximum is reached at collision energies which are somewhat greater

than the height of the potential barrier in the p -wave. As the collision energy grows further, the electron screening becomes less significant. As a result, the curves obtained in all the three versions of the calculation are almost coincident at $E > 1$ eV. In this region, there is one more maximum at $E \approx 2.4$ eV. The transfer rate is about $5 \times 10^{10} \text{ s}^{-1}$ at this energy. This maximum is due to a resonance behaviour of the partial contribution of the g -wave (Fig. 4). It is interesting to note that the height of the potential barrier in this wave is about 9 eV (Table 6), so that this resonance is deep-subbarrier.

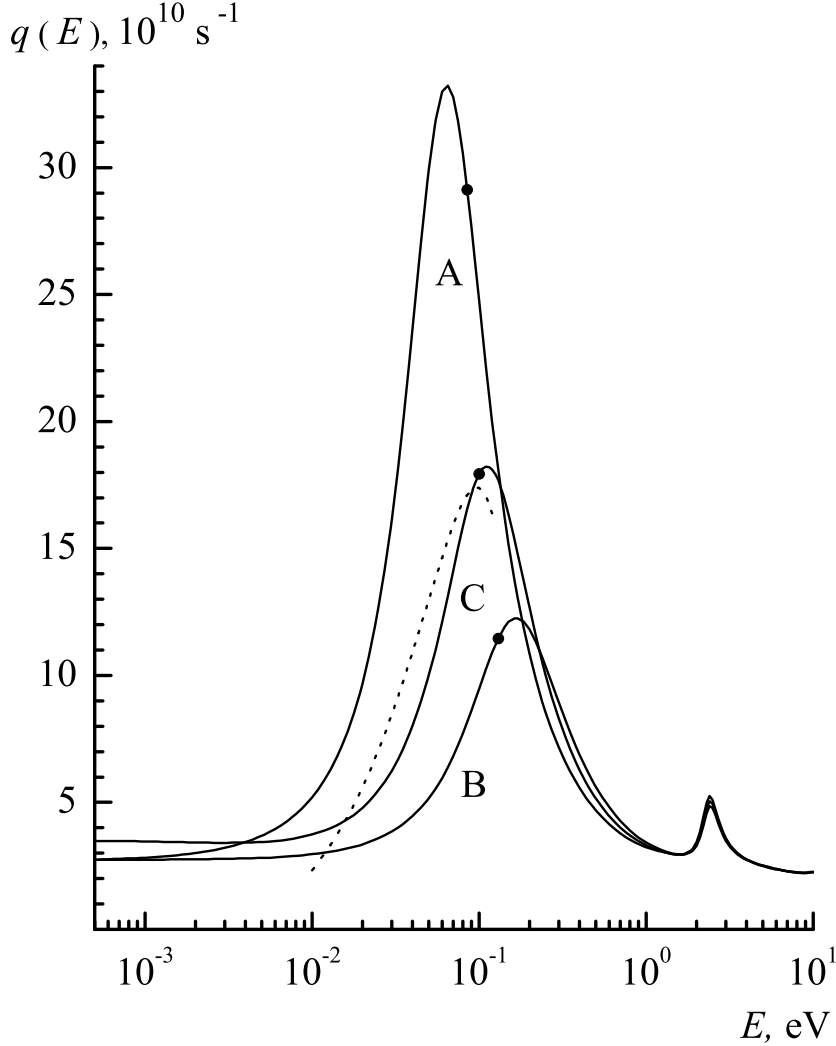


Figure 3: Muon transfer rate $q(E)$ versus the collision energy E . The solid curves represent the results obtained within the versions A, B, and C. The black circle on each curve indicates the value of E which is equal to the height of the barrier in the effective potential energy for the p -wave (Table 6). The dotted curve represents the experimental dependence of $q(E)$. It was calculated by the formula (4) with the central values of the coefficients from Table 2.

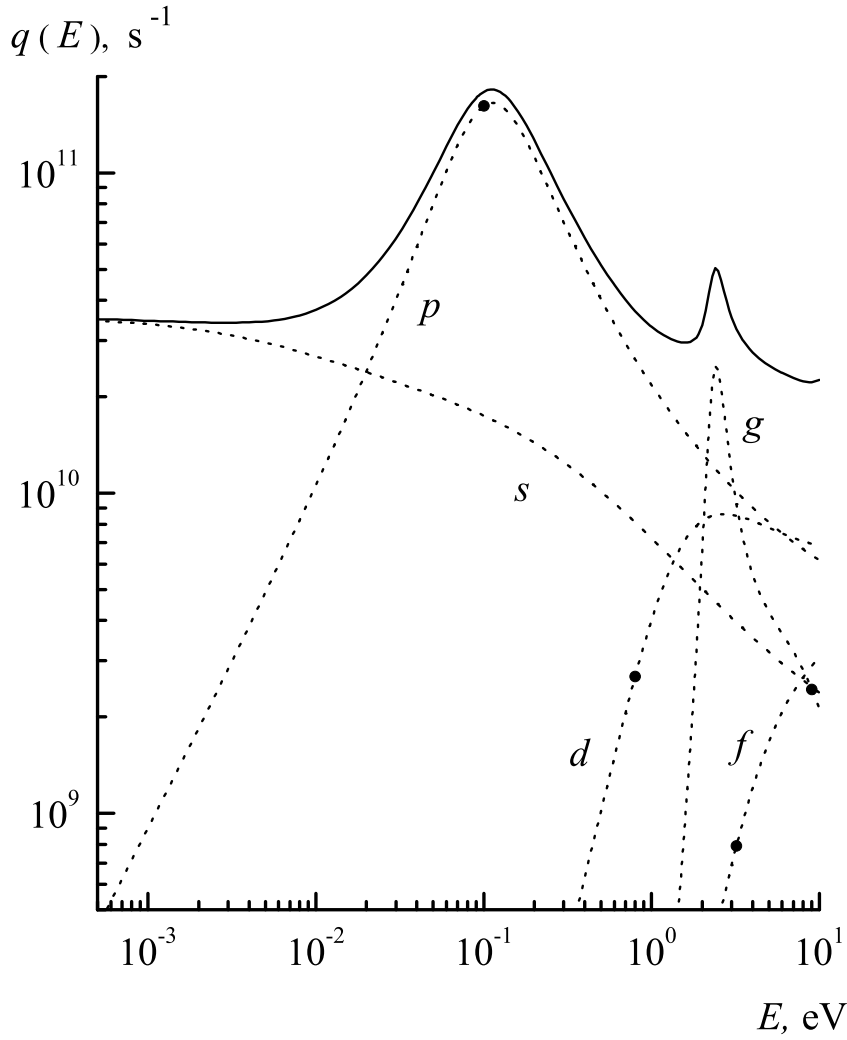


Figure 4: Partial muon tranfer rates versus the collision energy E . The curves were calculated within the version C. The solid curve represents the total transfer rate $q(E)$, the dotted curves are the contributions of the partial waves from s to g . The black circle on each dotted curve indicates the value of E which is equal to the height of the barrier in the effective potential energy for the respective partial wave (Table 6).

Table 7: Position E_m of the resonance maxima in the energy dependence of the muon transfer rate at collision energies $E < 1$ eV. q_m is the maximum transfer rate. The last row is the results of the approximation proposed in Ref. [5] (the formula (4) with the central values of the coefficients from Table 2).

Version of calculation	E_m , eV	q_m , 10^{11} s^{-1}
A	0.0640	3.32
B	0.167	1.23
C	0.112	1.82
[5]	0.0972	1.74

The experimental curve of the dependence $q(E)$ is also shown in Fig. 3. It was obtained in Ref. [5] as a result of the processing of data on the temperature dependence of the transfer rate. This curve was calculated by the formula (4) with the central values of the coefficients from Table 2. The position and the height of the maximum of this curve are given in Table 7. In the region of $E > 0.015$ eV, the curve calculated within the version C agrees well with the experimental curve. The calculated and experimental values of the position of the maximum and its height are also close. At lower collision energies, the agreement becomes worse. It is possible that this is due to molecular effects. In this context, two circumstances should be noted.

1. The logic of the present calculation is that the muon transfer occurs at interatomic distances R not exceeding 24 muon–atom units. This value is about one tenth of the electron Bohr radius, and it is noticeably less than dimensions of the oxygen molecule. At greater values of R , the muonic hydrogen atom moves in the spherically symmetric field of the free oxygen atom. Actually, the molecular field is much more complicated. In particular, it is not spherically symmetric. It is natural to expect that this fact may be significant at low collision energies.
2. The nuclei of the oxygen molecule take part in internal vibrational–rotational motion. In particular, there are zero–point vibrations at any temperature. Their consideration may be also important at low collision energies.

Let us now consider the temperature dependence of the rate $\lambda(T)$ of the muon transfer from thermalized muonic hydrogen atoms. For a collision of the muonic atom with a free oxygen atom, this quantity is obtained by averaging the rate $q(E)$ over the Maxwellian distribution of relative velocities in the entrance reaction channel. The results are presented in Fig. 5, in Table 8, and also in Appendix B. In all the three versions of the calculation, the transfer rate increases monotonically with temperature. This results from the growth of the rate $q(E)$ at thermal collision energies. The best agreement with experimental data is obtained in the version C. At $T > 150$ K, the calculated curve lies somewhat lower than experimental points. Its deviations from these points do not exceed 15 %. At lower temperatures, the agreement is poorer. The calculated values become greater than the experimental ones, and at $T \leq 104$ K exceed the latter by 30 – 40 %. This fact may also be an indication of the need to take into account molecular effects.

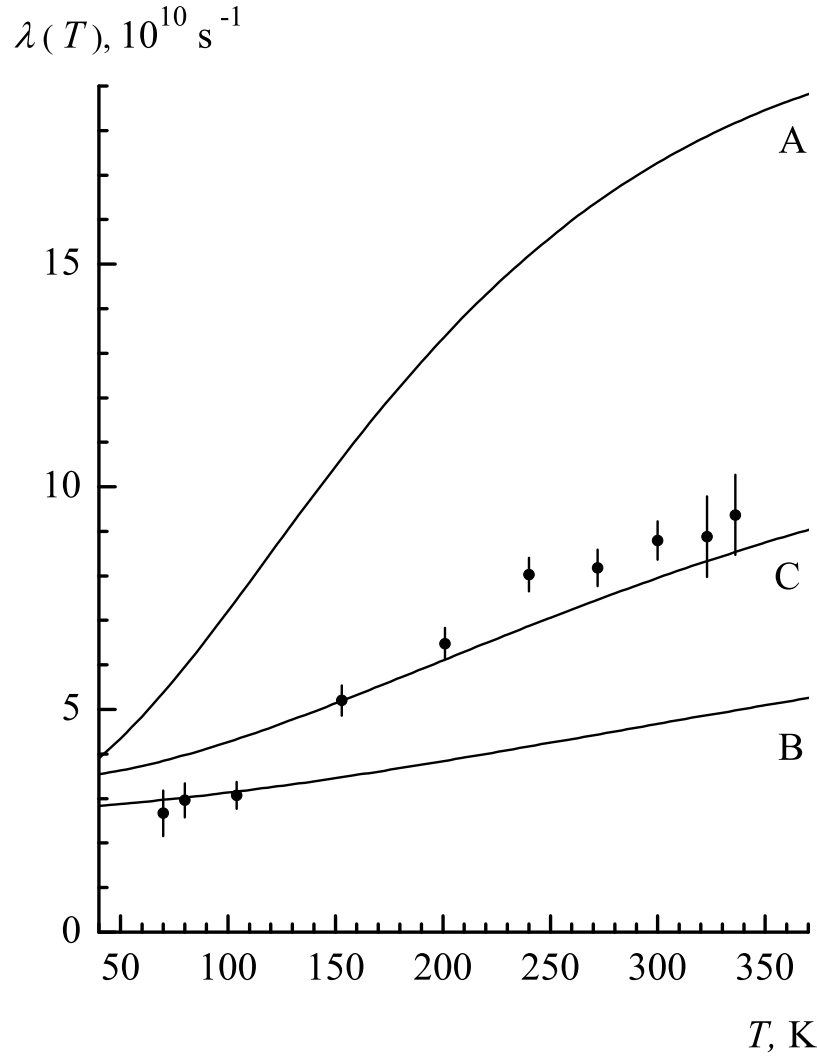


Figure 5: Rate $\lambda(T)$ of the muon transfer from thermalized muonic hydrogen atoms versus temperature. The solid curves represent the results obtained within the versions A, B, and C. The black circles are the experimental values obtained in Refs. [6, 7] (Table 8).

Table 8: Experimental λ_{exp} and calculated λ_{th} values of the rate $\lambda(T)$ of the muon transfer from thermalized muonic hydrogen atoms to oxygen at various temperatures. All the rates are given in units of 10^{10} s^{-1} . The experimental values were taken from Refs. [6, 7]. The errors were calculated by the formula $\sigma = \sqrt{\sigma_1^2 + \sigma_2^2}$, where σ_1 and σ_2 are given in Table 1. The values of λ_{th} were calculated within the versions A, B, and C.

$T, \text{ K}$	λ_{exp} [6, 7]	λ_{th}		
		A	B	C
70	2.67 ± 0.51	5.38	2.97	3.84
80	2.96 ± 0.38	5.96	3.02	3.97
104	3.07 ± 0.30	7.47	3.16	4.33
153	5.20 ± 0.34	10.6	3.48	5.19
201	6.48 ± 0.35	13.4	3.85	6.12
240	8.03 ± 0.38	15.2	4.17	6.87
272	8.18 ± 0.41	16.4	4.44	7.47
300	8.79 ± 0.43	17.3	4.68	7.95
323	8.88 ± 0.91	17.9	4.87	8.33
336	9.37 ± 0.90	18.2	4.98	8.54

In conclusion, let us review some results.

1. In the collision energy region of $0.015 < E < 0.1 \text{ eV}$, the calculated values of the transfer rate agree well with the results obtained by the processing of experimental data. In particular, the calculation predicts the existence of a p -wave resonance at an energy of $E \approx 0.1 \text{ eV}$. This result seems to be important in the context of the planned laser experiment on precise measurements of the hyperfine splitting energy of the $1s$ state of muonic hydrogen.
2. At temperatures of $T \geq 150 \text{ K}$, the calculated values of the rate of the muon transfer from thermalized muonic atoms are also in good agreement with experimental values.
3. The results of the calculation are quite sensitive to the electron screening. Good agreement with experimental data is obtained only with its proper consideration.
4. As the collision energy decreases to 0.01 eV and the temperature decreases to 100 K , the agreement between calculated and experimental values becomes poorer. A possible reason may lie in molecular effects.

Appendix A

Tables given below represent numerical values of the muon transfer rate $q(E)$ calculated for a number of collision energies E within the versions A, B, and C.

E , eV	$q(E)$, 10^{10} s^{-1}		
	A	B	C
1×10^{-4}	2.70	2.74	3.54
2×10^{-4}	2.71	2.74	3.53
4×10^{-4}	2.73	2.73	3.51
6×10^{-4}	2.76	2.74	3.49
8×10^{-4}	2.79	2.74	3.47
1×10^{-3}	2.82	2.74	3.46
2×10^{-3}	3.00	2.75	3.42
4×10^{-3}	3.44	2.80	3.41
6×10^{-3}	3.95	2.85	3.48
8×10^{-3}	4.54	2.90	3.59
0.01	5.20	2.96	3.74
0.015	7.19	3.14	4.21
0.02	9.68	3.35	4.79
0.025	12.7	3.59	5.47
0.03	16.1	3.85	6.24
0.035	19.9	4.14	7.09
0.04	23.6	4.46	8.01
0.045	27.1	4.80	8.99
0.05	29.9	5.17	10.0
0.055	31.9	5.56	11.1
0.06	33.0	5.96	12.1
0.065	33.2	6.39	13.1
0.07	32.8	6.82	14.1
0.075	31.8	7.27	15.0
0.08	30.6	7.72	15.9
0.085	29.1	8.17	16.6
0.09	27.6	8.61	17.1
0.093	—	—	17.4
0.095	26.2	9.05	17.6

$E, \text{ eV}$	$q(E), 10^{10} \text{ s}^{-1}$		
	A	B	C
0.1	24.8	9.47	17.9
0.105	—	—	18.1
0.11	22.2	10.2	18.2
0.115	—	—	18.2
0.12	20.0	10.9	18.1
0.125	—	—	17.9
0.13	18.1	11.5	17.7
0.135	—	—	17.4
0.14	—	—	17.1
0.145	—	—	16.7
0.15	15.2	12.1	16.3
0.16	—	—	15.6
0.17	13.1	12.3	14.8
0.18	—	—	14.0
0.2	10.9	11.8	12.7
0.22	—	—	11.5
0.25	8.57	10.4	10.0
0.3	7.17	8.94	8.30
0.35	6.24	7.78	7.12
0.4	5.57	6.88	6.27
0.45	5.07	6.17	5.64
0.5	4.69	5.62	5.15
0.6	4.14	4.82	4.47
0.7	3.78	4.28	4.01
0.8	3.53	3.89	3.70
0.9	3.36	3.62	3.47

$E, \text{ eV}$	$q(E), 10^{10} \text{ s}^{-1}$		
	A	B	C
1.0	3.24	3.42	3.31
1.2	3.07	3.15	3.10
1.5	2.96	2.97	2.96
1.7	2.97	2.96	2.96
1.9	3.18	3.10	3.13
2.0	3.43	3.29	3.35
2.1	3.85	3.60	3.71
2.2	4.42	4.07	4.23
2.3	4.99	4.57	4.76
2.4	5.25	4.85	5.04
2.5	5.10	4.79	4.94
2.6	4.75	4.51	4.63
2.7	4.37	4.18	4.28
2.8	4.05	3.90	3.97
2.9	3.79	3.67	3.73
3.0	3.59	3.49	3.54
3.2	3.30	3.22	3.26
3.5	3.02	2.97	3.00
4.0	2.77	2.74	2.75
5.0	2.51	2.50	2.51
6.0	2.38	2.37	2.37
7.0	2.29	2.29	2.29
8.0	2.24	2.24	2.24
9.0	2.23	2.22	2.22
10.0	2.26	2.25	2.25

Appendix B

Tables given below represent numerical values of the rate $\lambda(T)$ of the muon transfer from thermalized muonic hydrogen atoms for a number of temperatures T . These values were calculated within the versions A, B, and C.

$T, \text{ K}$	$\lambda(T), 10^{10} \text{ s}^{-1}$		
	A	B	C
20	3.17	2.77	3.45
25	3.33	2.79	3.46
30	3.51	2.80	3.48
35	3.70	2.82	3.51
40	3.90	2.84	3.55
45	4.11	2.86	3.58
50	4.34	2.88	3.63
55	4.59	2.90	3.68
60	4.84	2.92	3.73
65	5.11	2.95	3.79
70	5.38	2.97	3.84
75	5.67	2.99	3.91
80	5.96	3.02	3.97
85	6.27	3.05	4.04
90	6.58	3.07	4.11
95	6.89	3.10	4.19
100	7.21	3.13	4.27
110	7.86	3.19	4.43
120	8.52	3.25	4.59
130	9.17	3.32	4.77
140	9.82	3.39	4.95
150	10.5	3.46	5.14
160	11.1	3.53	5.33
170	11.7	3.60	5.52
180	12.2	3.68	5.71
190	12.8	3.76	5.91
200	13.3	3.84	6.10

$T, \text{ K}$	$\lambda(T), 10^{10} \text{ s}^{-1}$		
	A	B	C
210	13.8	3.92	6.30
220	14.3	4.00	6.49
230	14.8	4.08	6.68
240	15.2	4.17	6.87
250	15.6	4.25	7.06
260	16.0	4.34	7.25
270	16.3	4.42	7.43
280	16.7	4.51	7.61
290	17.0	4.59	7.78
300	17.3	4.68	7.95
310	17.5	4.76	8.12
320	17.8	4.84	8.28
330	18.0	4.93	8.44
340	18.3	5.01	8.60
350	18.5	5.09	8.75
360	18.6	5.18	8.89
370	18.8	5.26	9.03
380	19.0	5.34	9.17
390	19.1	5.42	9.30
400	19.3	5.49	9.43

-
- [1] L.D. Landau and E. M. Lifshitz, *Quantum Mechanics*(Pergamon, 1977), sections 143 and 121.
 - [2] A. Werthmüller *et al.*, Hyperf. Interact. **116**, 1 (1998).
 - [3] A. Adamczak, D. Bakalov, K. Bakalova, E. Polacco, and C. Rizzo, Hyperf. Interact. **136**, 1 (2001).
 - [4] D. Bakalov, A. Adamczak, M. Stoilov, and A. Vacchi, Phys. Lett. A **379**, 151 (2015).
 - [5] E. Mocchiutti *et al.*, arXiv: 1905.02049 v1 [nucl-ex] 6 May 2019.
 - [6] E. Mocchiutti *et al.*, Phys. Lett. A **384**, 126667 (2020).
 - [7] C. Pizzolotto *et al.*, Phys. Lett. A **403**, 127401 (2021); arXiv: 2105.06701 v1 [physics.atom-ph] 14 May 2021.
 - [8] S. S. Gershtein, Sov. Phys. JETP, **16**, 501, (1962).
 - [9] R. A. Sultanov and S. K. Adhikari, Phys. Rev. **A62**, 022509 (2000).
 - [10] V. I. Savichev and R. Blümel, Eur. Phys. J. **D21**, 3 (2002).
 - [11] A. Dupays, Phys. Rev. Lett. **93**, 043401 (2004).
 - [12] A. Dupays, B. Lepetit, J. A. Beswick, C. Rizzo, and D. Bakalov, Phys. Rev. **A69**, 062501 (2004).
 - [13] Anh–Thu Le and C. D. Lin, Phys. Rev. **A71**, 022507 (2005).
 - [14] S. V. Romanov, Eur. Phys. J. **D28**, 11 (2004).
 - [15] S. V. Romanov, Phys. At. Nucl. **77**, 1 (2014).
 - [16] K. Kobayashi, T. Ishihara, and N. Toshima, Muon Cat. Fusion **2**, 191 (1988).
 - [17] I. V. Komarov, L. I. Ponomarev, and S. Yu. Slavyanov, *Spheroidal and Coulomb Spheroidal Functions* (Nauka, Moscow, 1976), pp. 15–17, 171–178, 190–196 [in Russian].
 - [18] G. Jaffé, Z. Phys. **87**, 535 (1934).
 - [19] W. G. Baber and H. R. Hassé, Proc. Cambr. Phil. Soc. **31**, 564 (1935).
 - [20] D. R. Bates and T. R. Carson, Proc. Roy. Soc. **A234**, 207 (1956).
 - [21] Gisèle Hadinger, M. Aubert-Frécon, and Gerold Hadinger, J. Phys. **B22**, 697 (1989).
 - [22] A. S. Davydov, *Quantum Mechanics* (Pergamon, 1965), sections 43 and 107.
 - [23] A. V. Kravtsov, A. I. Mikhailov, and N. P. Popov, J. Phys. **B19**, 1323 (1986).
 - [24] E. Clementi and C. Roetti, At. Data Nucl. Data Tables **14**, 177 (1974).